Journal of Natural Science Review

Vol. 4, No. 1, 2026
https://kujnsr.com
e-ISSN: 3006-7804

Comparative Depth-Dose Analysis for Prostate Cancer BNCT Using MIT and BMRR Epithermal Neutron Spectra Reactors

Rajab Ali Khavari[1*], Dawood Mirzaee[2], Noor Mohammad Azizi[3], Ihsanul Haq Yar[4]

[1] Physics and Electronics Department, Faculty of Physics, Kabul University, Kabul, Afghanistan
[2] Nuclear and Atomics Department, Faculty of Physics, Kabul University, Kabul, Afghanistan
[3] Nuclear and Atomics Department, Faculty of Physics, Kabul University, Kabul, Afghanistan
[4] Physics and Electronics Department, Faculty of Physics, Kabul University, Kabul, Afghanistan

[*]E-mail: khavary81@gmail.com (corresponding author)

ABSTRACT

This research concentrated on dose assessments for boron neutron capture therapy (BNCT) as a possible definitive treatment for prostate cancer. BNCT functions by precisely targeting boron-10 (^{10}B) to cancerous cells, which, when they absorb thermal neutrons, emit high-energy particles—primarily alpha particles and lithium nuclei—that destroy tumor cells while preserving adjacent healthy tissue. This study assessed the depth-dose distribution within the prostate tumor and adjacent tissues using Monte Carlo simulations with the MCNP and Geant4 codes. These instruments simulate the motion and interactions of neutrons and secondary particles in tissue to accurately predict dose distributions. The simulations employed epithermal neutron spectra from the MIT and BMRR reactors, which are ideal for BNCT, as epithermal neutrons can penetrate deeper into tissue before slowing to thermal energies where boron-10 capture occurs. The findings indicated that the boron-10 concentration, neutron flux, and the configuration of the epithermal neutron spectrum highly influence the depth-dose within the prostate. The estimated total dose in the prostate was 0.03–0.08 (Gy/s). The research additionally measured the dose and energy distributions of secondary particles generated during nuclear interactions, which are crucial for evaluating tumor control and effects on normal tissue. The results suggest that BNCT holds considerable promise as a treatment for prostate cancer, providing precise tumor irradiation and minimizing harm to adjacent tissues.

ARTICLE INFO

Article history:

Received: October 22, 2025
Revised: November 18, 2025
Accepted: February 10, 2026
Published: March 31, 2026

Keywords:

BNCT Method; Depth-dose; Epithermal neutron spectrum; MIT Reactor; Monte Carlo computational code; Prostate cancer; SRIM

To cite this article: Khavari, R. K., Mirzaee, D., Azizi, N. M & Haq Yar, I. (2026) Comparative depth-dose analysis for prostate cancer BNCT using MIT and BMRR epithermal neutron spectra reactors. *Journal of Natural Science Review, 4* (1), 315-334. *https://doi.org/10.62810/jnsr.v4i1.302*
Link to this article: https://kujnsr.com/JNSR/article/view/302

INTRODUCTION

As of 2011, prostate cancer ranked as the second most frequently identified cancer and the sixth leading cause of cancer-related deaths among men worldwide (Baade et al., 2009; Jemal et al., 2011). In the United States, it ranks second. Radiation therapy usually plays an essential role in the treatment of prostate cancer and, in many instances, is the only option available (Siegel et al., 2011). In relation to these cancers, radiation commonly refers to X-rays; however, recent research has shown encouraging results for the use of epithermal neutrons in boron neutron capture therapy (BNCT) (Yasui et al., 2012; Wolber, 2004; Wagner et al., 2012). The idea of neutron absorption theory was first proposed in 1936 by J. L. Locher,

and its application has continued in various methods and for various purposes (Hawthorne & Lee, 2003; IAEA, 2001; Gambarini et al., 2008). Although BNCT demonstrated promise for cancer treatment, it often fell short because of the uncertain state of the tumor within the surrounding tissue. The BNCT technique has significantly improved the management of Glioblastoma and various forms of human brain tumors (Savolainen et al., 2013). The BNCT clinical trial began in 1951 and was founded by W. H. Sweet and his associates (Nakagawa, 2001). The laboratory tests employing the BNCT technique yielded disappointing results due to insufficient boron compounds, leading to a pause from 1961 until 1968, when H. Hatanaka in Japan achieved significant results. Following Hatanaka's notable achievement, the United States and various European countries began clinical trials of the BNCT technique (Allen, 2006).

The BNCT method significantly improved treatment for Glioblastoma and various forms of human brain tumors (Savolainen et al., 2013). No practical or clinical studies have been conducted on treating the prostate gland using BNCT. Nevertheless, comprehensive research is currently underway using various methods, including BNCT, to treat the prostate gland (Khavari & Mirzaee, 2024). The BNCT method is being utilized and studied for prostate gland treatment at various scientific research centers, including accredited institutions such as the University of Tsukuba in Japan (Yamamoto et al., 2011; Yamamoto et al., 2004), the University of Birmingham in England (Hamidi & Scott, 2002), the Cancer Institute of New Mexico, and the International Cancer Institute in the United States. The MIT Reactor Research Center in the U.S. provides unique facilities for BNCT and is the only center in the country permitted to conduct human clinical trials.

The boron neutron therapy method aims to eradicate cancer cells, requiring that the energy uptake in the tumor be much higher than in normal tissue. As a result, the boron-10 isotope is introduced into the patient's system via the BSH ($Na_2B_{12}H_{11}SH$) medication; BSH concentrates in the nuclei of cancer cells, while its uptake in healthy tissues is limited. This explains why it is used in neutron therapy, which presently has many applications (Allen, 2006). To treat tumors located at depths of 2 to 5 cm with the BNCT approach, an epithermal neutron source is required to provide an adequate flux. Reactors are located near the sources producing the epithermal neutron beam at a suitable flux (Auterinen et al., 2004).

As a result of interactions with surrounding organs, the epithermal neutrons become thermal and are absorbed by boron-10 before reaching the cancerous gland. The excited atoms of (^{11}B) break apart, releasing an alpha particle (^{4}He) and a rebounding (^{7}Li) atom. The cross-section for this reaction is substantial for thermal neutrons (3837 barn); in 93.7% of instances, the energies of the alpha particle and (^{7}Li) ion are 1.48 MeV and 0.84 MeV, with their ranges in water measuring 7.2 pm and 4.1 pm, correspondingly (Ogawara et al., 2020) . As a result, the energy released from this reaction occurs at a scale comparable to cell sizes. Because of their high LET and RBE, these particles can cause double or multiple DNA breaks, which reduces the DNA repair capabilities of cancer cells (Nakia et al., 2014; Zhu et al., 2024). Moreover, these precisely targeted energy-delivery events predominantly affect tumor cells

while sparing adjacent healthy tissue. BNCT can improve the radiotherapy approach as, firstly, the secondary particles created by this method demonstrate a LET (linear energy transfer) that is 5 to 50 times higher than the radiation generated by electron and proton accelerators in medical centers (Wagner et al., 2012), and secondly, the neutron beam spectrum production in BNCT is more economical in comparison to Hadron therapy (Barth et al., 2012; Dymova et al., 2020; George et al., 2010).

Computational phantoms are essential for determining the dose from external irradiation in BNCT because of their simple design and ease of incorporation into Monte Carlo codes, which increases their effectiveness. The mathematical concepts of quadratic equations and CGS (constructive geometry) are employed to pinpoint the organs and body outlines within the simulation. This type of phantom, known as the ORNL family of models, is one of the most common methods for assessing tissue dose from external radiation (Krstic & Nikezic, 2007) . In BNCT, the external neutron beam interacts with tissues as it travels, resulting in absorbed dose in the surrounding healthy tissues. The total dose and depth-dose analysis were calculated and modeled utilizing the two Monte Carlo codes, MCNPX and Geant4. Several essential subjects were analyzed in simulations conducted with Monte Carlo computational codes to enhance BNCT for treating the prostate gland: 1- The most significant therapeutic benefit arises when boron levels in the prostate gland exceed those in the surrounding healthy tissue. Sure, please provide the text you'd like me to paraphrase. 2- Due to the prostate gland's location at a depth of less than 5 cm, an appropriate epithermal neutron beam with the proper energy and flux is required.

Given that the prostate gland is located less than 5 cm from the body's surface, an improved BNCT method is necessary to target it with neutron beams of appropriate energy and flux. The present study evaluated the total dose received by the prostate and neighboring organs using the ORNL-MIRD computational phantoms; furthermore, the depth-dose within the prostate and adjacent tissues was progressively examined and calculated.

MATERIALS AND METHODS

The male adult model used in the simulations is part of the ORNL computational phantom series, which is ideal for calculating external radiation doses (Krstic & Nikezic, 2011). While the ICRU and ICRP commissions suggested various compositions to enhance alignment with actual anatomy (ICRP, 2003) , the standard models of the MIRD phantoms recognize only the three tissue types of bone, lung, and soft tissue. To achieve more realistic modeling, 19 distinct tissues, along with their compositions and densities, were considered and simulated per ICRU 46 (ICRUM, 1992) for the MIRD phantom using both computational codes. In this research, following the MIRD 15 edition, the prostate gland was included in the ORNL-MIRD phantom (1996), modeled as a sphere with a radius of 2 cm. According to ICRP 89 (Auterinen et al., 2004), there is a 2 cm gap between the outer surface of this sphere and the skin, which was simulated using MCNPX and Geant4 (GEANT 4 team, n.d.), the two Monte Carlo simulation codes. The MCNPX Monte Carlo computational code, version 2.6, is regarded as

the primary code for dose calculations in the prostate and adjacent tissues in the present study.

The Geant4 Monte Carlo code is used to verify the MCNPX results, and a comparison of their computations is conducted. An additional reason for employing GEANT calculations is the transport of (^{7}Li) ions and (^{4}He) particles. The cutoff energies for the (^{7}Li) ion and (^{4}He) particle in MCNPX exceed their energies generated from neutron capture by (^{10}B). Consequently, the MCNPX code cannot transport these particles at such low energies, whereas this study primarily targets the transport of charged particles at low energy for prostate gland treatment via the BNCT method. In this study, the distance traversed by the (^{7}Li) ion and (^{4}He) particle computations was assessed and executed using a different Monte Carlo program, SRIM-2013 (Ziegler, 2013). Since the epithermal neutron beam source is external, the cumulative dose in various organs, including the prostate, and the depth-dose in the phantom were examined and computed incrementally (1 mm per mesh) in simulations, in accordance with the macroscopic dimensions of the sample.

The Epithermal Neutron Source

Table 1*: Range Allowed Radiation exposure to method in BNCT*

Neutron beam parameters required for BNCT	Range of parameters
ϕ_{epi}	$[n/cm^2 - s]1E+10^9 <$
ϕ_{epi}/ϕ_{fast}	> 20
ϕ_{epi}/ϕ_{ther}	> 100
ϕ_{fast}/ϕ_{epi}	$[Gycm^2/n]2E-13 >$
D_{gama}/ϕ_{epi}	$[Gycm^2/n]2E-13 <$
Fast neutrons	$E_n > 10keV$
Epithermal neutrons	$10keV < E_n < 1eV$
Thermal neutrons	$E_n < 1eV$

Table 2 shows the parameter values for the MIT and BMRR reactors utilized in this research. These values may be contrasted with the BNCT allowable irradiation limits listed in Table 1.

Table 2: *Parameters of reactor neutron spectrum specifications for MIT and BMRR in boron neutron capture therapy*

Reactor	University	Power (MW)	ϕ_{epi} $10^9[n/cm^2 - s]$	ϕ_{fast}/ϕ_{epi} $10^{-13}[Gycm^2/n]$	D_{gama}/ϕ_{epi} $10^{-13}[Gycm^2/n]$
MIT	USA	5	3.71	1	3.6
BMRR	USA	3	0.88	2.7	1.3

Tables (1) and (2) indicate that both reactors have acceptable irradiation thresholds for the BNCT (Tung et al., 2004; Wang et al., 2022). Therefore, for dosimetric calculations, the epithermal neutron spectra from the BMRR and MIT reactors were obtained and modeled individually as external beam irradiation of the body.

MCNPX2.6 Monte Carlo code

The F6:n, F6:p, and F6:e tally cards were used to obtain the dose for each particle delivered to different organs the MCNPX code (McKinney et al., 2008). The +F6 tally card was utilized to determine the total dose in every cell of the simulated phantom. In the simulations, the F6 tally card concept refers to the average absorption energy per particle as it moves through a

cell, and its unit is MeV/g in the Monte Carlo code. In contrast, the +F6 tally card in simulations reports the average absorption energy calculated from all particles that move within a specific cell and/or volume. The two tally cards, F4:p and F4:e, along with the E4 energy card, were employed independently at specified energy ranges to determine the energy spectrum of secondary particles generated in nuclear interactions, where the F4 tally card represents the average flux of particles moving through each cell, measured in MeV/cm². The mesh tally card was used to compute the depth-dose (mesh operates in mm units) within the phantom depth. The average absorption energy resulting from the transported particle in each source of the phantom cells is determined using the initial mesh tally in this card, which can be equivalent to the F6 tally card. The third category of the mesh tally card is used to determine the depth-dose from all particles transmitted through the phantom depth, which can be regarded as the +F6 tally card.

The Geant4 Monte Carlo Computational code

A geometry similar to that used in the MCNPX code was also implemented in the GEANT4 code. Data extraction in Geant4 is achieved through three methods: scoring mesh, sensitive detector, and the third, user hooks, which is utilized for dose calculation in this study (GEANT4 Coll., 2010) . The user hooks method consists of five classes: G4 User Run Action, G4 User Event Action, G4 User Tracking Action, G4 User Stepping Action, and G4 User Stacking Action. Based on their attributes, these categories are used to determine the dose in simulations. Consequently, the G4 User Stepping Action class is employed to compute the dose within the tissue cells and the dose of the secondary particles incrementally. Various models are implemented in the Geant4 computational code for electromagnetic and nuclear interactions. The energy spectrum in electromagnetic models spans from 1 keV to 10 V (Ivanchenko et al., 2011). Depending on their application, these designs are divided into two categories: high-energy and low-energy. This project has employed the two models of Livermore physics and Penelope physics, both classified as low-energy models, as the standard models are mainly associated with high energy and, in addition, rely on mathematical computations. This research utilizes both the Livermore and Penelope physics models. As both are for low-energy applications and use ICRU 73 experimental data in these models, the dose estimates across different cells are more accurate (Amako et al., 2005).
The nuclear physics models encompass Binary Cascade and Bertini Cascade; Binary Cascade serves as the nuclear model for interactions involving light ions, and this sample configuration in Geant4 is an intra-nuclear cascade intended to replicate the interactions of protons, neutrons, and ions with atomic nuclei. This model was applied to nuclear interactions in the study (Floger et al., 2004).

Boron Concentrations in the Prostate Gland

The majority of the absorbed dose in the BNCT technique comes from neutron capture by boron. Consequently, variations in boron levels in the tissue would primarily influence the dose received and the selection of the treatment model. Furthermore, the accumulation of the BSH drug occurs not only in cancerous cells but also in some healthy tissues. Therefore,

when these normal tissues are exposed to thermal neutrons, they will absorb a significant amount of radiation. This situation arises in many tissues next to tumors positioned along the neutron beam. The presence of (^{10}B) in tumor tissues (at varying concentrations) and its distribution in both normal and cancerous tissues with different levels has been examined. Boron levels in tumor tissues are 3 to 10 times greater than in the normal tissues adjacent to the tumor (Mirzaee et al., 2014; Nievaart V. A. et al., 2007; Koivunoro, 2012). Consequently, the boron concentration in prostate tumor tissue, according to sources (Joensuu et al., 2003; Viaggi et al., 2004; Blue & Yanch, 2003; Nievaart V. A. et al., 2007) , was modeled at levels of 15 ppm and 30 ppm, whereas the distribution of (^{10}B) is presumed to present at a concentration of 5 ppm in healthy tissues like the skin, soft tissues surrounding tumors, bladder, kidneys, and testicles, which receive the highest dose.

FINDINGS

All data were computed with a relative error of less than 0.1%. The simulation results indicated that (^{4}He) at 60% and (^{7}Li) at 30% were the most significant contributors to the dose delivered in prostate cancer (ZHou et al., 2025), while the remaining dose was associated with other secondary particles generated during nuclear interactions. Because the concentration of boron-10 in prostate cancer is greater than in nearby healthy tissues, the dose experienced in those tissues is significantly lower. Consequently, the ratio of the dose delivered to prostate cancer compared to the surrounding healthy tissues is 9.9 (Karimzadeh et al., 2024). The energy spectra in various body tissues, including prostate gland tissue, were examined to highlight the significance of secondary particle transport. The charged particles, alpha and lithium, lack a spectrum because they are single-energy; therefore, the energy spectra of secondary particles, including photons and electrons, in the different tissues of the phantom were analyzed, as illustrated in Figure 1.

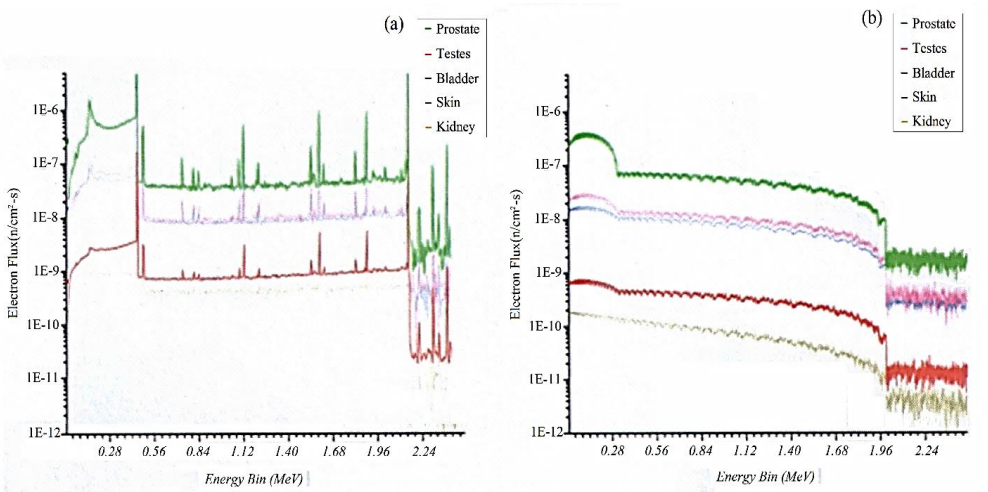

Figure 1. *Energy distribution of secondary particles (a) photons and (b) electrons generated in nuclear interactions*

The distinct peaks of these secondary particles at specific energies indicate that their maximum concentration in tissues occurs within this energy range; hence, their dosage needs to be assessed in the prostate gland and nearby tissues at these energy levels. This research is significant because it analyzes the epithermal neutron spectrum from active reactors as the framework for the neutron treatment method involving boron. It examines the total dose from alpha particles, lithium, and other secondary particles generated in nuclear interactions within internal organs, particularly the prostate gland, which is treated as cancerous tissue (Khavari & Mirzaee, 2024).

Table 3. *Overall dosage in the prostate gland exceeding BNCT epithermal neutron spectrum reactors Active BMRR and MIT*

Reactor	Flux reactor, the order of $[\times 10\ (n/cm^2\ .s)]$	Total dose by taking the flux and the concentration of 30 ppm boron-10(Gy/s)	
		MCNPX	Geant4
MIT	3.71	0.006	0.006341
BMRR	0.88	0.00149	0.001392

The overall quantity of secondary radiation from the surrounding tissues of the prostate gland, including the bladder, kidneys, skin, and testicles, which are at a higher risk of receiving the greatest dose, was also computed (Table 4). Calculating the dose in these organs is crucial as they are adjacent to the prostate gland and define its boundaries (Kissel et al., 2024).

Table 4. *Overall dose in the prostate gland and adjacent tissues subjected to the maximum radiation for varying concentrations using a spectrum from the MIT Reactor (Gy/s)*

Boron-10 concentration in the prostate gland	Prostate	Testes	Bladder	Skin	Kidneys
30ppm	6E-3	88E-8	12E-9	70E-10	10E-11
15ppm	3.6E-3	95E-8	13E-9	73E-10	12E-11

Table 4: Overall radiation dose in the prostate gland and adjacent tissue subjected to the maximum exposure for various concentrations using a spectrum from MIT Reactor (Gy/s).

The outcomes of the depth will be analyzed in two distinct sections: the depth-dose distributions in the prostate gland and adjacent tissues, obtained from the MCNPX and GEANT4 simulations separately.

Outcomes of the Total Dose and Depth-Dose Distribution Achieved from the MCNPX Code.

Figure 2 illustrates the two-dimensional representation of the physical depth-dose distribution. This illustration distinctly shows the depth-dose relationship based on the (^{10}B) concentration and the neutron spectrum shape. The illustration indicates that as the B-10 concentration elevates in the prostate, the dose escalates in the prostate tissue and diminishes in surrounding tissues, especially the skin (Mushtaq et al., 2023; Mirzaee et al., 2014). The dose distribution is distinctly visible in panels (a), (c), (b), (d) of Figure 2, where the epithermal neutron spectrum of the BMRR reactors served as the source for the first. In contrast, the epithermal neutron spectrum of the MIT reactors served as the source for the latter in all simulations. In Figure 2, the boron levels in the prostate are 15 ppm and 30 ppm in parts a and b, respectively, and 5 ppm in all adjacent tissues across all simulation programs.

The comparison of depth-dose distributions between a and b, as well as c and d, demonstrates how the dose distribution in various tissues depends on the boron levels within

the prostate gland. The dose distribution in skin tissues also increases as the concentration in the prostate gland decreases. When boron levels decline in the prostate gland, the accumulation of thermal neutrons increases in adjacent healthy tissues (Lee et al., 2009). The comparisons in parts (a), (c) and (b), (d) of Figure (2) demonstrate that the reactor spectrum shape is highly efficient in dose generation; this figure shows that the prostate gland will receive a greater dose if the epithermal neutron spectrum has the correct form and flux (MIT) as illustrated in parts (a), (c) of Figure 2.

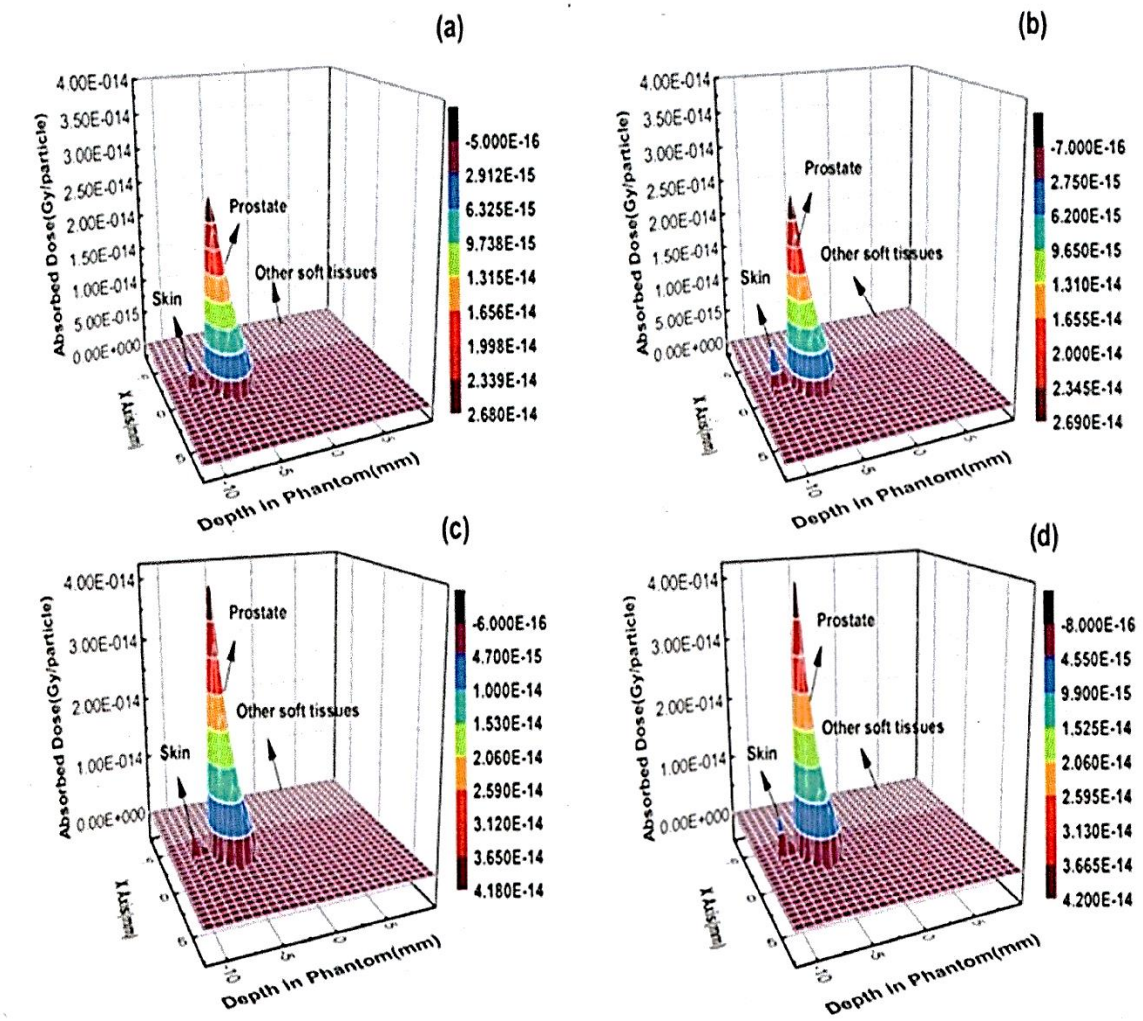

***Figure 2**: Illustrating the dose distribution in the two-dimensional section (a), (c) the depth dose distribution for the 30 and 15 ppm levels of boron-10 with the epithermal neutron spectrum from the MIT reactor and section (b), (d) the depth dose distribution for the 30 and 15 ppm levels of boron-10 with the epithermal neutron spectrum from the BMRR reactor*

Figure 3 shows the one-dimensional depth-dose distribution for the two specific concentrations, 15 ppm and 30 ppm, to more effectively demonstrate the significant dependence of boron neutron capture therapy techniques on boron concentrations. Be aware that with a rise in boron concentration, the dose distribution within the prostate gland becomes excessively high. In contrast, the dose distribution in adjacent tissues remains nearly unchanged at both concentrations (Mirzaee et al., 2014).

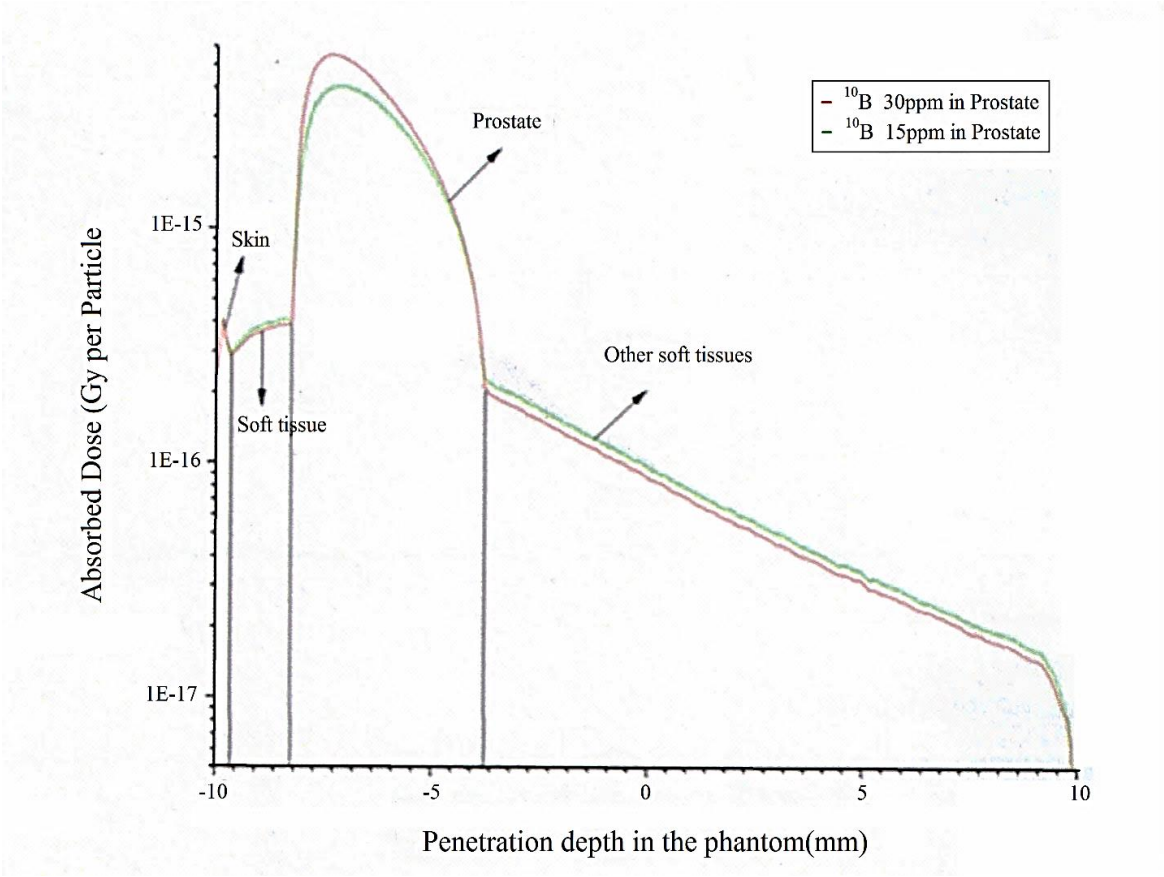

***Figure 3**: Illustrating the depth dose distribution for 30 and 15 ppm concentrations of boron-10 in prostate tissue and 5 ppm boron-10 in all tissues using the thermal neutron source reactor at MIT*

The epithermal neutron flux directly influences the treatment of prostate cancer using BNCT; as the reactor's epithermal neutron flux increases, the treatment becomes less effective because more thermal neutrons reach the prostate cancer in a shorter time. The quantity of neutrons generated by the MIT and BMRR reactors is 1678×10^9 and 398×10^9 n, respectively. Neutron production in the MIT reactor is estimated to be nearly four times that in the BMRR reactor. Consequently, a greater dose will reach prostate cancer more swiftly from the epithermal neutron spectrum of the MIT reactor; hence, a lower dose will affect the nearby healthy tissues during treatment compared to when using the neutron flux from the BMRR reactor (Mirzaee et al., 2014).

Outcomes of the Total Dose and the Depth-Dose Distribution Obtained from the Geant4 Code.

The Geant4 code was used to analyze and calculate the depth-dose distribution in the prostate gland and adjacent tissues to verify the MCNPX code results, as presented in Figure 4.

Figure 4 illustrates the depth-dose for boron-10 concentrations of 15 and 30 ppm in prostate gland tissue and 5 ppm in adjacent tissues around the prostate gland. Sections (a) and (c), along with sections (b) and (d) of Figure 4, illustrate the one-dimensional and two-dimensional dose distributions for boron-10 concentrations of 15 and 30 ppm within the

prostate tissue, respectively. The impact of varying boron-10 concentrations on the depth-dose distribution is evident in Figure 4, which shows that the highest dose is observed at higher boron-10 concentrations in the prostate tissue. The figure's two-dimensional representation clearly shows that as concentration rises, the dose in the prostate gland increases while it decreases in regions close to the source, resulting in a minimal dose there (Khavari & Mirzaee, 2024; Marcello et al., 2020). This study focuses on analyzing and quantifying the dose distribution of alpha particles generated in nuclear interactions; consequently, Figure 4 illustrates the calculation of the depth-dose distribution in the prostate gland and adjacent tissues from alpha particles at varying boron concentrations within the prostate gland. These outcomes are identical to those achieved using the MCNPX Monte Carlo computation code.

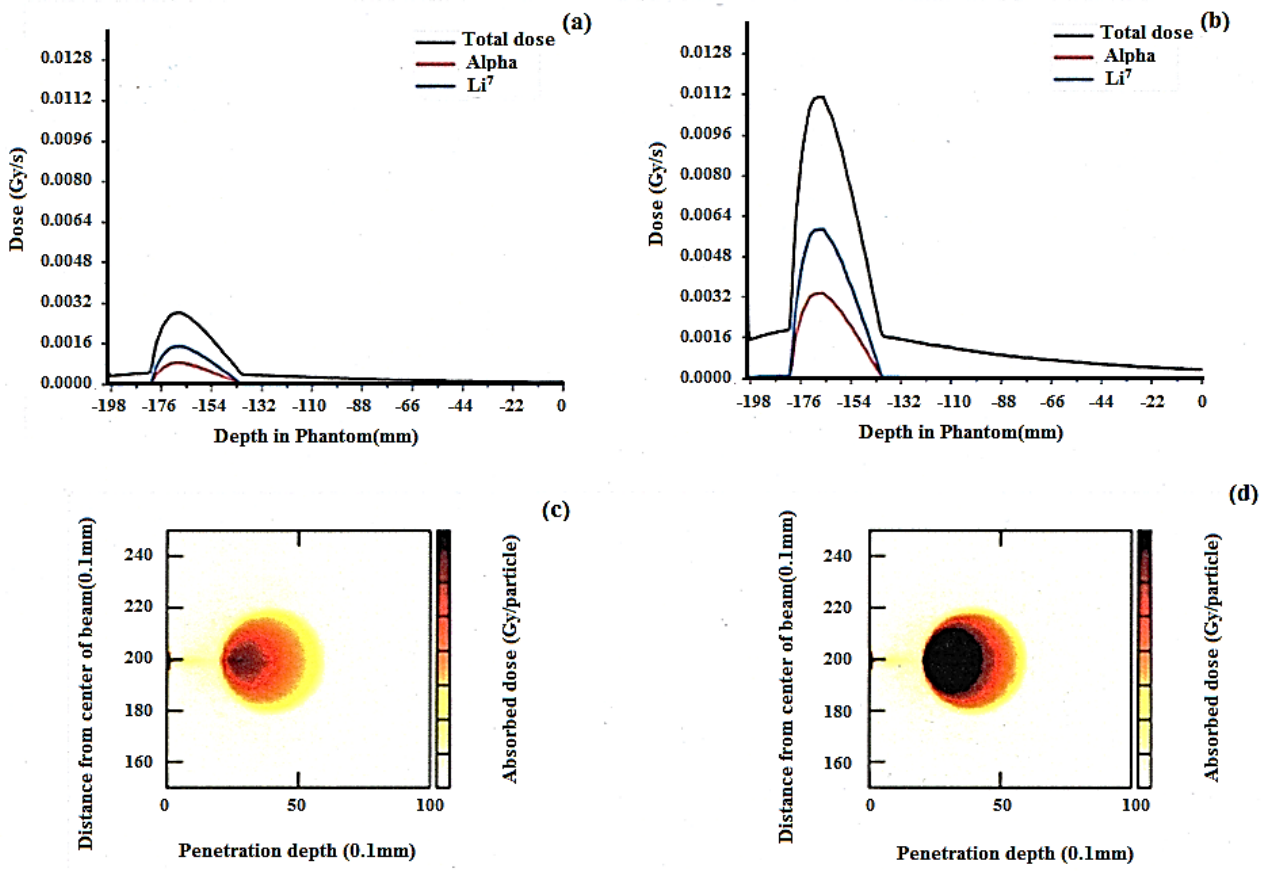

Figure 4*: The Geant4 Monte Carlo code illustrates the variation in depth-dose for a 30 ppm concentration of boron-10 in the prostate with various neutron sources (BMRR and MIT reactors). Sections (a) and (c) illustrate the one- and two-dimensional dose from the epithermal neutron spectrum of reactor BMRR, whereas sections (b) and (d) depict the one- and two-dimensional dose from the epithermal neutron spectrum of reactor MIT*

Figure 5 illustrates the logarithmic representation of depth dose along with the doses of secondary particles produced: alpha, lithium, neutrons, and photons in the interactions of nuclear epithermal neutrons with boron. It is evident here that the charged particles alpha and lithium cause the highest dose in the prostate gland. This study uses the BNCT method to demonstrate the dose distributions from the charged particles alpha and lithium within the prostate gland.

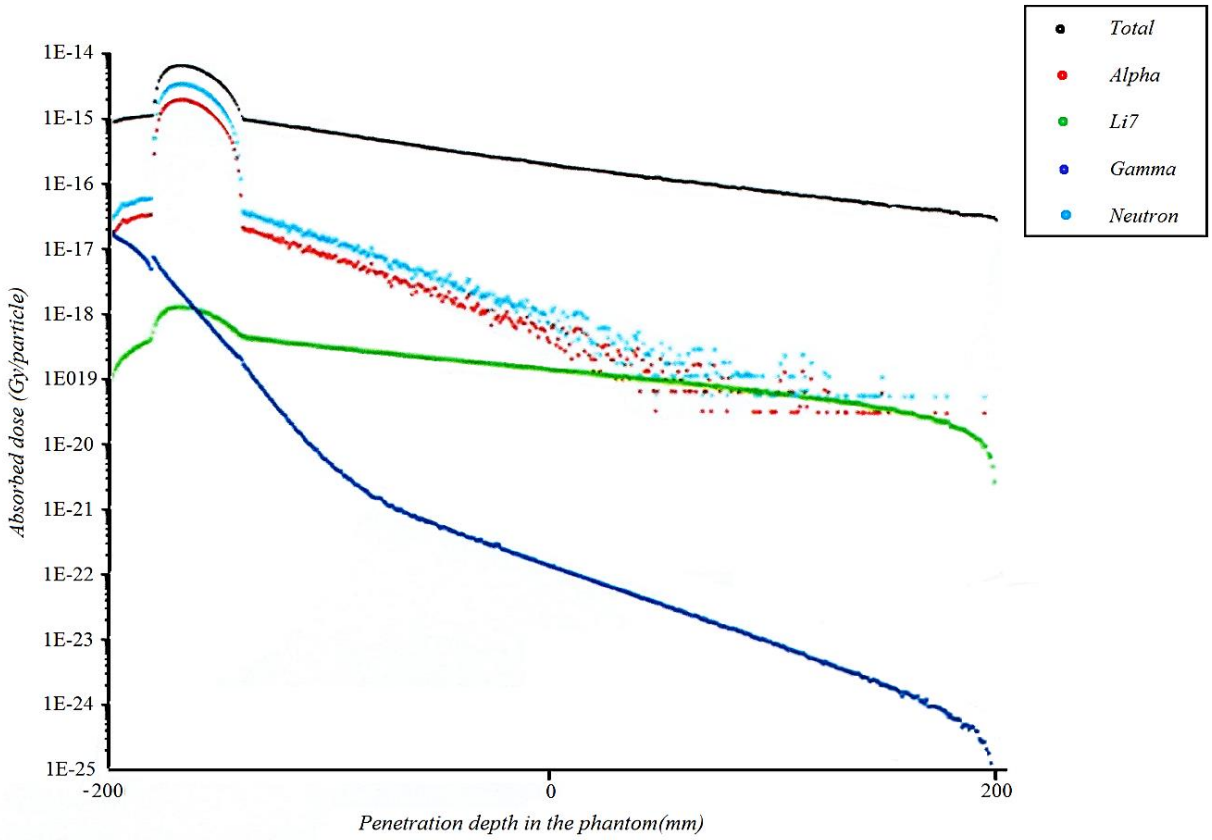

***Figure 5**: Illustrating the logarithmic depth dose of secondary particles generated from nuclear interactions in prostate tissue and within the tissues of the constructed phantoms*

DISCUSSION

This study emphasizes the significant impact of secondary particle dose in Boron Neutron Capture Therapy (BNCT). It offers a comprehensive evaluation of dose distribution, LET features, and treatment enhancement for prostate cancer utilizing an epithermal neutron beam. Secondary particles produced from nuclear interactions—particularly from the (10)B(n, α)(7)Li reaction—account for much of the biological efficacy of BNCT owing to their elevated linear energy transfer (LET). As highlighted by Pedrosa-Rivera et al. (2025), these secondary particles possess short ranges and high energies, allowing them to deliver a significant localized dose to tissues rich in (10)B. This analysis extends that concept by examining the effects of boron concentration, neutron spectral characteristics, and irradiation conditions on total and depth-dependent doses in the prostate and adjacent healthy tissues.

A key result of this study is the validation that the greatest absorbed dose in the prostate happens when the boron concentration is significantly higher than that of surrounding normal tissues. This aligns with the core therapeutic mechanism of BNCT: the selective increase in dose at the cellular level relies on attaining much higher boron absorption in tumor cells. The simulation findings indicate that a boron concentration ratio of roughly 1:1 between cancerous and adjacent tissues results in minimal dose variation. In contrast, higher tumor-

to-normal tissue uptake ratios significantly enhance the therapeutic index. This aligns with earlier studies indicating that inadequate boron selectivity may lower tumor control probability and increase the risk of normal tissue complications. Thus, the capacity to achieve sufficient boron accumulation is a crucial factor influencing the clinical success of BNCT. The article referenced below supports the findings reached (Chen et al., 2025).

The research further demonstrates the significant reliance of dose distribution on the characteristics of the epithermal neutron beam. Epithermal neutrons are favored for deep-seated tumors, such as those in the prostate, since they can penetrate tissue before thermalizing to energies better suited for the boron capture reaction. The significance of a suitably shaped spectrum with ideal flux is emphasized here: a properly crafted epithermal beam enhances penetration depth while also decreasing irradiation duration. Shortening irradiation time directly helps protect healthy tissue, as extended beam exposure elevates the impact of non-selective neutron-induced dose components (Deist & Gorissen, 2016).

The simulated beam conditions in this research produced a neutron flux level that facilitated the swift delivery of the therapeutic dose, guaranteeing that the tumor experienced optimal dose deposition from high-LET α particles and (^{7}Li) ions, while reducing excess exposure to healthy tissues. In BNCT, shaping the beam is essential for managing the ratio of epithermal, fast, and thermal neutrons; the current findings validate that a spectrum with reduced high-energy fast neutrons and increased epithermal content results in improved dose distributions (Lee et al., 2004) . Fast neutrons lead to unwanted high-LET background doses and have longer ranges, spreading the dose beyond the intended target area. In contrast, epithermal neutrons undergo thermalization at depth, enhancing dose conformity in the prostate—a crucial factor for targeted dose administration in BNCT.

The biological efficacy of BNCT relies on secondary particles with high linear energy transfer (LET). The recent results indicate that these particles play a major role in both the overall absorbed dose and the LET-weighted dose in the prostate. The limited range of α particles (~5–10 μm) ensures that damage is confined to specific cancer cells with high boron concentrations. This leads to fatal, clustered DNA damage that the cell struggles to repair. The simulations show that the depth-dose profile reflects the microscopic distribution of boron rather than the macroscopic distribution of neutron flux, indicating that BNCT operates differently from traditional external-beam radiotherapy. In standard photon therapy, the dose distribution relies heavily on beam attenuation within the tissue. In BNCT, the dosage is determined by the rate of nuclear reactions occurring locally within cells containing boron.

A further important finding from this research is the significance of regulating LET and its spatial arrangement. High-LET radiation is recognized for enhancing relative biological effectiveness (RBE) due to its compact ionization pattern. BNCT naturally generates mixed radiation fields, comprising high-LET elements from boron capture reactions and low-LET elements from gamma rays and scattered neutrons. The data show that the $\alpha/(\ ^{7}Li)$ component prevails in the tumor but has a minimal impact on surrounding tissues because of

the restricted range of these particles. In contrast, the dose outside the tumor is more affected by gamma rays and scattered neutrons but stays considerably lower than inside the tumor when boron concentration is optimized. This specific distribution underscores the conceptual benefit of BNCT for treating tumors where varying boron uptake is possible.

The current study's exploration of depth-dependent dose indicates that the overall administered dose decreases with increasing distance from the prostate center, consistent with anticipated neutron attenuation and reduced boron reaction rates. Crucially, the simulations show that healthy organs, like the bladder and rectum, are exposed to significantly lower doses when boron levels in these tissues are maintained at physiological or minimal levels. This corresponds with current experimental findings indicating that normal tissues with reduced boron absorption undergo significantly fewer boron-capture occurrences, thereby decreasing high-LET exposure. The results thus reinforce the belief that BNCT can achieve better dose conformity than traditional radiotherapy techniques, which frequently have difficulty minimizing collateral dose to at-risk organs near the prostate.

A notable result of this study concerns the interaction among irradiation duration, beam quality, and dosimetric effectiveness. Reduced irradiation durations enhance patient comfort and alleviate logistical challenges while also lessening the impact of non-boron-associated dose factors. As shown by Deist and Gorissen (2016), the duration of treatment is a crucial factor in the overall risk assessment of radiotherapy processes, especially for beams that generate mixed particle fields. High-performance beam-shaping systems that optimize the production of epithermal neutrons significantly improve the clinical viability of BNCT for deep-seated tumors. The findings validate that improving flux and spectral characteristics shortens irradiation durations while maintaining therapeutic dose levels.

The findings further enhance understanding of secondary particle physics in BNCT. Secondary particles produced from neutron scattering (such as recoil protons and gamma rays) add to the background dose. However, their contribution is relatively minor compared to the boron-capture component when boron levels are elevated (Donya et al., 2025). This emphasizes the importance of boron pharmacokinetics and drug-delivery methods. Achieving significant tumor selectivity remains a challenge in BNCT research, and upcoming studies may investigate improved boron carriers with enhanced tumor uptake, such as nanoparticles, porphyrin derivatives, and molecular targeting agents.

Although the positive results of this research are encouraging, several limitations must be acknowledged. Initially, simulations rely heavily on assumptions about the uniformity of boron distribution, even though in vivo distributions may be variable. Secondly, the research assumes optimal beam conditions that may differ from those of existing clinical neutron sources. Differences in beam-shaping assembly efficiency, clinical accelerator output, or patient anatomy may alter dose distributions. Third, the factors of biological effectiveness (such as Compound Biological Effectiveness and Relative Biological Effectiveness) were not directly modeled in this instance but are crucial for converting physical dose into clinical

impact (Kreiner et al., 2014). Including these factors would offer a broader assessment of therapeutic potential.

Nonetheless, the results hold significant clinical relevance. Prostate cancer continues to be a significant cancer worldwide, and treatment options like photon radiotherapy, proton therapy, and brachytherapy frequently encounter difficulties in attaining both effective tumor control and low toxicity (Barth et al., 2018). BNCT, due to its ability to deliver a higher dose to the cellular level, offers a promising alternative—especially in situations where standard treatments have not succeeded or where tumor recurrence necessitates re-irradiation. The high-LET characteristics of secondary particles provide a biological benefit in eliminating radioresistant tumor cells. Additionally, customizing boron levels and neutron spectra offers possibilities for personalized treatment strategies (Barth et al., 2018).

Future research paths include enhancing boron-delivery techniques to improve tumor selectivity, advancing accelerator-based neutron sources for broader clinical use, and incorporating BNCT dose calculations into multimodality treatment planning frameworks. Furthermore, a more thorough examination of LET spectra and microdosimetric effects might provide deeper insight into biological reactions. Clinical trials concentrating on prostate BNCT will be crucial for confirming simulation results and developing treatment protocols.

Safety management in BNCT is crucial, as it involves overseeing dose to healthy tissues and managing boron absorption. Combination therapies using radiotherapy or chemotherapy can enhance effectiveness, yet regulatory limitations and accessibility to neutron sources continue to pose clinical challenges and necessitate standardization and safety verification.

CONCLUSION

Research and computations on dose distribution within the prostate gland and nearby organs show that the absorbed dose in the prostate tissue is influenced by the concentration of boron-10 in both the prostate and adjacent healthy tissues, as well as by the flux and characteristics of the neutron source spectrum (epithermal neutrons). The results indicate that when the flux exceeds a specific threshold, the absorbed dose in the healthy tissues surrounding the prostate gland will increase, while it will decrease within the prostate gland due to proton recoil. Nonetheless, if the intensity is high, the dose distribution within the prostate will exceed that in the surrounding areas. Calculations indicated that the maximum depth-dose in prostate gland tissue was achieved by increasing the boron concentration in the cancerous tissue; a dose range of 0.08-0.3 (Gy/s) was determined. Based on assessments of the depth-dose calculation in prostate gland tissue, one recommendation is to clarify whether the neutron source spectrum in the BNCT method has the correct intensity and shape. Subsequently, the concentration of boron-10 within the prostate gland tissue, acting as a neutron attractant, must be maximized relative to the surrounding normal tissues, ensuring that thermal neutrons are primarily concentrated in the prostate tissue owing to

boron's high absorption cross-section. As a result of boron nuclear interactions with thermal neutrons, secondary particles such as alpha and lithium will be produced more frequently, leading to the highest dose in the prostate tissue due to their inherent properties.
Additionally, the prostate's proximity to the source is crucial to consider, as the epithermal neutron spectrum may become ineffective beyond a specific threshold. In the boron neutron capture therapy technique, if the distance from the source to the cancer tissue exceeds the threshold, then sources must be used that lack sufficient energy and flux. As previously noted, if the source has low energy and flux, only a small number of thermal neutrons reach the cancer tissue, resulting in a low dose within the tissue. Thus, depending on the tumor's location, it is essential to carefully select the energy, flux, and configuration of the neutron source. Assessment of the depth-dose using the two Monte Carlo simulation codes MCNPX and Geant4 (Figs. 4, 5 for comparison) in this research indicates that the outcomes would be significantly improved and more favorable if the BNCT approach is combined with other techniques for treating prostate cancer in the examined conditions.

AUTHORS CONTRIBUTIONS

Every author made contributions in various sections, and each played a significant role in the completion of this article, detailed below:

- Dawood Mirzaee handles data gathering and coding for Monte Carlo and GIANT4 simulations. This information is a component of his doctoral dissertation.
- Data collection and source review are the responsibilities of Ihsanul Haq Yar and Noor Mohammad Azizi.
- Rajab Ali Khavari (corresponding author) took charge of examining the results and contrasting them with the latest published studies.
- The full team of writers oversaw the final editing of the piece and authorized its release.

ACKNOWLEDGEMENTS

Members of the author's team carried out the data collection and analysis, with no other individuals participating.

FUNDING INFORMATION

There are no funds available for the manuscript.

CONFLICT OF INTEREST STATEMENT

The authors state that there are no conflicts of interest.

DATA AVAILABILITY STATEMENT

The preliminary findings are taken from the thesis, presented as a simulation, and all comparison and review sources are accessible online at no cost.

REFERENCES

Allen, B. J. (2006). Internal high linear energy transfer (LET) targeted radiotherapy for cancer. *Phys Med Biol., 51*(13), 327-41. https://doi.org/10.1088/0031-9155/51/13/R19

Amako, K., Guatelli, S., Ivanchenko, V. N., & Maire, M. (2005). Comparison of Geant4 Electromagnetic Physics Models Against the NIST Reference Data. *IEEE Transactions on Nuclear Science, 52*(4), 910-18. https://doi.org/10.1109/TNS.2005.852691

Auterinen, I., Seren, T., Antilla, K., Kosunen, A., & Savolinen, S. (2004). Measurement of free beam neutron spectra at eight BNCT facilities worldwide. *Appl Radi & Isop., 61*(5), 1021-26. https://doi.org/10.1016/j.apradiso.2004.05.035

Baade , P. D., Youlden, D. R., & Krnjacki, L. J. (2009, feb). International epidemiology of prostate cancer: geographical distribution and secular trends. *Molecular nutrition&food research, 53*(2), 171-84. https://doi.org/doi:10.1002/mnfr.200700511

Barth, R. F., Mi, P., & Yang, W. (2018). Boron delivery agents for neutron capture therapy of cancer. *Cancer Commun (Lond), 38*(1), 1-15. https://doi.org/doi: 10.1186/s40880-018-0299-7.

Barth, R. F., Vicente, M. H., Harling, O. K., Kinger 3rd, W., & Riley, K. J. (2012, Aug). Current status of boron neutron capture therapy of high grade gliomas and recurrent head and neck cancer. *Radiat Oncol, 7*(146). https://doi.org/10.1186/1748-717X-7-146

Blue, T. E., & Yanch, J. C. (2003). Accelerator-based epithermal neutron sources for boron neutron capture therapy of brain tumors. *Journal of Neuro-Oncology, 62*(1-2), 19-31. https://doi.org/10.1007/BF02699931

Chen, Y., Zheng, Q., Wang, B., Peng, H., Tang, Y., Zhang, X., . . . Li, Z. (2025). Research on the dose calculation of BNCT based on the time-varying boron concentration in pharmacokinetics. *J Radiat Res., 66*(6), 627-637. https://doi.org/DOI: 10.1093/jrr/rraf038

Deist, T. M., & Gorissen, B. L. (2016). High-dose-rate prostate brachytherapy inverse planning on dose-volume criteria by simulated annealing. *Physics in Medicine & Biology, 61*(1155). https://doi.org/DOI 10.1088/0031-9155/61/3/1155

Donya, H., Alzahrani, N. M., Abdulsalam, A., & Umer, M. (2025, Aug). Boron neutron capture therapy: a promising radiation treatment modality. *Radiat Environ Biophys, 64*(3), 339-353. https://doi.org/DOI: 10.1007/s00411-025-01134-2

Dymova, M. A., Taskaev, S. Y., Richter, V. A., & Kuligina, E. V. (2020). Boron neutron capture therapy: Current status and futureperspectives. *Cancer Communications., 40*, 406-421. https://doi.org/DOI: 10.1002/cac2.12089

Floger, G., Ivanchenko, V., & Wellish, J. (2004). The Binary Cascade. *The European Physical Journal A - Hadrons and Nuclei, 21*, 407-17. https://doi.org/10.1140/EPJA%2FI2003-10219-7

Gambarini, G., Breskin, A., & Battistoni, G. (2008). Studies of a gamma-blind fast-neutron imaging detector for BNCT applications. Anno Accademico.

GEANT 4 team. (n.d.). *https://geant4-userdoc.web.cern.ch/UsersGuides/PhysicsReferenceManual/html/index.html*. (GEANT 4)

GEANT4 Coll. (2010). *Geant4 User's Guide for Application Developers:Version geant4 9.4.* York University.

George, S., Roeske, C. J., McDevitt, M. R., & Palm, S. (2010). MIRD Pamphlet No. 22 (abridged): radiobiology and dosimetry of alpha-particle emitters for targeted radionuclide therapy. *Journal of Nuclear Medicine, 51*(2), 311-328. https://doi.org/10.2967/jnumed.108.058651

Hamidi, S., & Scott, M. C. (2002, jan). BNCT neutron beam characterization using a resonance absorption filter method. *nuclear instruments and methods in physics research section a:accelerators,spectrometers,detectors-and-associated-equipment, 476*(1-2), 99-105. https://doi.org/10.1016/S0168-9002(01)01399-7

Hawthorne, M. F., & Lee, M. W. (2003, mar). A critical assessment of boron target compounds for boron neutron capture therapy. *Journal of neutron oncology, 62*(1-2), 33-45. https://doi.org/10.1007/BF02699932

IAEA. (2001). *Current Status of Neutron Capture Therapy.* VIENNA: IAEA.

ICRP. (2003). Basic Anatomical and Physiological Data for Use in Radiological Protection Reference Values. *Ann ICRP, 32*(3-4), 5-265.

ICRUM. (1992). *Photon, electron, proton and neutron interaction data for body tissues.* MD USA: ICRUM Bethesda.

Ivanchenko, V., Apostolakis, j., Bagulya, A. V., & Abdelouahed, H. B. (2011). Recent Improvements in Geant4 Electromagnetic Physics Models and Interfaces. *PROGRESS IN NUCLEAR SCIENCE AND TECHNOLOGY, 2*, 898-03. https://doi.org/10.15669/pnst.2.898

Jasim, B. I., Elias, N. Y., Hassoun, H. A., Issa, R. A., & Mahmood, Y. H. (2025). *Introduction to Radiological Physics and Radiation Dosimetry.* Delhi: Bright Sky Publicashions. https://doi.org/ https://doi.org/10.62906/bs.book.364

Jemal, A., Bray, F., Melissa, C. M., Ferlay, J. M., Elizabeth, W., & David, F. (2011, feb). Global cancer statistics. *CA:A Cancer Journal for Clinicians, 61*(2), 69-90. https://doi.org/10.3322/caac.20107

Joensuu, H., Kankaanranta, K., Auterinen, I., Kallio, M., Kulvik, M., & Laakso, J. (2003). Boron neutron capture therapy of brain tumors: clinical trials at the finnish facility using boronophenylalanine. *Journal of Neuro-Oncology, 62*(1-2), 123-34. https://doi.org/10.1007/BF02699939

Karimzadeh, A., Schatz, L., Sasur, M., Apostolova, I., Buchert, R., Klutmann, S., & Lehnert, W. (2024). Organ and tumor dosimetry including method simplification for [177Lu]Lu-PSMA-I&T for treatment of metastatic castration resistant prostate cancer. *EJNMMI Phys, 11*(63). https://doi.org/doi: 10.1186/s40658-024-00668-6

Khavari, R. A., & Mirzaee, D. (2024). Using Lithium-6 Filter for Study of Dose Distribution with Max. and Min. Displacement of Prostate Inside the Body by BNCT Method. *cognizancejournal, 4*(4), 235-243. https://doi.org/DOI: 10.47760/cognizance.2024.v04i04.016

Kissel, M., Terlizzi, M., & Giraud, N. (2024). Prostate radiotherapy may cause fertility issues: a retrospective analysis of testicular dose following modern radiotherapy techniques. Radiat Oncol 19, 101 (2024). *Radiat Oncol, 19*(101). https://doi.org/https://doi.org/10.1186/s13014-024-02498-3

Koivunoro, H. (2012). Thesis: Dosimetry and dose planning in boron neutron Capture therapy: Monte Carlo studies. Helsinki Finland: Department of Physics, Faculty of Science, and University of Helsinki Finland.

Kreiner, A. J., Bergueiro, J., Cartelli, D., Baldo, M., Castell, W., Asoia, J. G., . . . Igarzabal, M. (2014, dec 12). Present status of Accelerator-Based BNCT. *Rep Pract Oncol Radiother, 21*(2), 95-101. https://doi.org/doi: 10.1016/j.rpor.2014.11.004

Krstic, D., & Nikezic, D. (2007). *Input files with ORNL - Mathematical phantoms of the human body for MCNP-4B,Computer Physics Communications, 176*(1), 33-37. https://doi.org/http://dx.doi.org/10.1016/j.cpc.2006.06.016

Krstic, D., & Nikezic, D. (2011). Debugging of ORNL Series of Mathematical Phantoms of Human Body. *Acta Physica Polonica A, 119*(3), 279-81. https://doi.org/10.12693/APhysPolA.119.279

Lee, D. J., Han, C. Y., Park, S. H., & Kim, J. K. (2004). An accelerator-based epithermal neutron beam design for BNCT and dosimetric evaluation using a voxel head phantom. *Radiat Prot Dosimetry, 110*(1-4), 655-60. https://doi.org/DOI: 10.1093/rpd/nch107

Lee, K. W., Wu, J. K., Jeng, S. C., & Lin, Y.-W. H. (2009). Skin Dose Impact from Vacuum Immobilization Device and Carbon Fiber Couch in Intensity Modulated Radiation Therapy for Prostate Cancer. *Medical Dosimetry, 34*(3), 228-32. https://doi.org/DOI:10.1016/j.meddos.2008.10.001

Marcello, M., Denham, J. W., Kennedy, A., Haworth, A., Steigler, A., Greer, P. B., . . . Ebert, M. A. (2020). Reduced Dose Posterior to Prostate Correlates With Increased PSA Progression in Voxel-Based Analysis of 3 Randomized Phase 3 Trials. *Int J Radiat Oncol Biol Phys, 108*(5), 1304-18. https://doi.org/doi: 10.1016/j.ijrobp.2020.07.030.

McKinney, G. W., Durkee, J. W., Fensin, M. L., Hendricks, J. S., & James, M. R. (2008, April). MCNPX 2.6.0, Monte Carlo All-Particle Transport Code System including MCNPDATA. *Los Alamos, NM: Los Alamos National Laboratory*.

Mirzaee, D., Mir-Hakimabad, H., & Rafat-Motawalli, L. (2014). Depth Dose evalution for prostate cancer treatment using boron neutron capture therapy. *Radional nulear chem., 302*, 1095-01. https://doi.org/doi:10.1007/s10967-014-3397-2

Mushtaq, S., Ji Ae, P., Kim, J. Y., Lee, J. C., & Kim, K. I. (2023). The role of radiolabeling in BNCT tracers for enhanced dosimetry and treatment planning. *Theranostic, 13*(15), 5247-65. https://doi.org/doi: 10.7150/thno.88998

Nakagawa, Y. (2001). *Clinical practice in BNCT to the brain.* Vienna: IAEA.

Nakia, K., Ymamoto, T., Kumada, H., & Matsumura, A. (2014). Boron Neutron Capture Therapy for Glioblastoma: A Phase-I/II Clinical Trial at JRR-4. *Eur Assoc Neuro Oncol Mag., 4*(3), 116-23. https://doi.org/https://www.kup.at/kup/pdf/12232.pdf

Nievaart, V. A., Moss, R. L., Kloosterman, J. K., J vander Hagen, T. J., van Dam, H., Wittig, A., & Malago, M. (2006). Design of a rotating facility for extracorporal treatment of an explanted liver with disseminated metastases by boron neutron capture therapy with an epithermal neutron beam. *Radiat Res., 166*, 81-88. https://doi.org/10.1667/RR3535.1

Nievaart, V. A., Moss, R. L., Kloosterman, J. L., van der Hagen, T. J., & van Dam, H. (2007). *Spectral Tailoring for Boron Neutron Capture Therapy.* UK: IOS Press.

Ogawara, R., Kusumoto, T., Konisha, T., Hamano, T., & Kodaria, S. (2020). Detection of alpha and 7Li particles from 10B(n, α)7Li reactions using a combination of CR-39 nuclear track detector and potassium hydroxide-ethanol-water solution in accelerator-based neutron fields. *Nuclear Instruments and Methods in Physics Research Section B: Beam Interactions with Materials and Atoms, 467*(15), 9-12. https://doi.org/https://doi.org/10.1016/j.nimb.2020.01.030

Pedrosa-Rivera, M., Praena, J., Ruiz-Ruiz, C., Ruiz-Magana, M. J., & Porras, I. (2025).). Neutron relative effectiveness factors in Boron Neutron Capture Therapy: Estimation of their values from the secondary charged particles and evaluation of weighted kerma factors for a standard tissue. *arxiv*. https://doi.org/. https://arxiv.org/abs/2501.17761

Savolainen, S., Kortesniemi, M., Timonen, M., Reijonen, V., & Kuusela, L. (2013, may). Boron neutron capture therapy (BNCT) in Finland: technological and physical prospects after 20 years of experiences. *Phys Med., 29*(3), 233-48. https://doi.org/10.1016/j.ejmp.2012.04.008

Siegel, R., Ward, E., Brawley, O., & Jemal Ahmedin. (2011, june). The impact of eliminating socioeconomic and racial disparities on premature cancer deaths. *CA:A Cancer Journal for Clinicians, 61*(4), 212-236. https://doi.org/10.3322/caac.20121

Tung, C. J., Wang, Y. L., Hsu, F. Y., Chang, S. L., & Liu, Y.-W. H. (2004). Characteristics of the new THOR epithermal neutron beam for BNCT. *Appl Radi & Isot, 61*(5), 861-64. https://doi.org/10.1016/j.apradiso.2004.05.066

Viaggi, M., Dagrosa, M. A., Longhino, J., Blauman, H., Calzeta, O., & Kahl, S. B. (2004). Boron neutron capture therapy for undifferentiated thyroid carcinoma:preliminary results with the combined use of BPA and BOPP. *Applied Radiation and Isotopes, 61*(5), 905-09. https://doi.org/10.1016/j.apradiso.2004.05.005

Wagner, f. M., Loeper-Kabasakal, B., & Breitkreutz, H. (2012). Neutron medical treatment of tumours - A survey of facilities. *Journal of Instrumentation, 7*(3). https://doi.org/10.1088/1748-0221/7/03/C03041

Wang, S., Zhang, Z., Miao, L., & Li, Y. (2022). Boron Neutron Capture Therapy: Current Status and Challenges. *Front Oncol., 12*. https://doi.org/DOI: 10.3389/fonc.2022.788770

Wolber, G. (2004). Fast Neutron Beams for Boron Neutron Capture Therapy? *Zeitschrift für Medizinische Physik, 14*(1), 5563. https://doi.org/https://doi.org/10.1078/0939-3889-00192

Yamamoto, A., Nakai, K., Nariai, T., Kumada, H., Okumura, T., & Mizumoto, M. (2011, feb). The status of Tsukuba BNCT trial: BPA-based boron neutron capture therapy combined with X-ray irradiation. *Appl Radiat Isot., 69*(12), 1817-1818. https://doi.org/10.1016/j.apradiso.2011.02.013

Yamamoto, T., Matsumura, A., Nakai, K., Shibata, Y., Endo, K., & Sakurai, F. (2004). Current clinical results of the Tsukuba BNCT trial. *Appl Radi & Isot., 61*(5), 1089-1093. https://doi.org/10.1016/j.apradiso.2004.05.010

Yasui, L., Kroc, T., Gladden, S., Androf, C., Bux, S., & Hosmane, N. (2012, jan). Boron neutron capture in prostate cancer cells. *Appl Radiat Isot., 70*(1), 6-12. https://doi.org/10.1016/j.apradiso.2011.07.001

ZHou, Z., Chen, Y., Wang, Y., Hong, Y., Guan, H., Huang, F., . . . Xu, B. (2025). 'Cell knife'for cancer: the cliniciann prespective. *16*. https://doi.org/• DOI: 10.3389/fimmu.2025.1536355

Zhu, Y., Zuo-Kang, L., Hai-Yan, y., Ye, D., Zhi-Min, D., & Xiao-Han, Y. (2024). Study on the optimal incident proton energy of 7Li(p, n)7Be neutron source for boron neutron capture therapy. *Nuclear Science and Techniques, 35*(3). https://doi.org/dOI:10.1007/s41365-024-01420-6

Ziegler, J. F. (2013). *http://www.srim.org/SRIM/SRIMLEGL.htm*. (SRIM)